Alexandria Engineering Journal (2022) 61, 4445–4455

HOSTED BY

Alexandria University

Alexandria Engineering Journal

www.elsevier.com/locate/aej
www.sciencedirect.com

Computational solutions for Eikonal equation by differential quadrature method

Mehrullah Mehr, Davood Rostamy *

Department of Mathematics, Imam Khomeini International University, Qazvin, Iran

Received 22 June 2020; revised 2 October 2021; accepted 3 October 2021
Available online 23 October 2021

KEYWORDS

Eikonal equation;
Wave Propagation;
Polynomial differential quadrature;
Fourier differential quadrature

Abstract This article presents an efficient method to solve of Eikonal equation by the new differential quadrature method. The purpose of this article is to obtain the accuracy and performance method for the Eikonal equation. We introduce a novel grid points to reduce errors and compared them on different issues to accelerate convergence. The accuracy and stability of numerical results for two and three-dimensional of the Eikonal equation are presented. In these numerical examples, we investigate the stability of the proposed method by adding random noises. The new differential quadrature method is a capable method for the some numerical examples and we evaluate the accuracy and performance of our proposed method.

© 2021 THE AUTHORS. Published by Elsevier BV on behalf of Faculty of Engineering, Alexandria University. This is an open access article under the CC BY-NC-ND license (http://creativecommons.org/licenses/by-nc-nd/4.0/).

1. Introduction

We consider the following equation,

$$\begin{cases} |\nabla u(x,y)| = f(x,y), & (x,y) \in \Omega \setminus \Gamma, \\ u(x,y) = g(x,y), & (x,y) \in \Gamma \subset \Omega, \end{cases} \tag{1}$$

where $f(x,y)$ is a known function and Γ is a source point. So Ω is a computational domain and Γ is a subset of Ω. In Eq. (1), $u(x,y) = g(x,y), (x,y) \in \Gamma$ is the boundary condition. This equation is known as Eikonal equation and many of scientist are involved in different fields of physics, especially geometric optics [54,34]. The Eikonal equation is very useful in many applications in light emission, radar, contact lenses, elastic waves, projectors, mirrors, etc. To understand the physical equation of Eikonal, the following formula can be considered. Let $\mathbf{E}$ is the electric field strength, and V is the electric potential then we have the following equation according to velocity potential in fluid flow and temperature in heat transfer:

$$\mathbf{E} = -\nabla V.$$

Its physical meaning in electromagnetic discussions is that it is pressed each time in the region to move from a right angle to the constant potential lines and along the lines of force determined by the vector **E**and the sign. Therefore, the functions in (1) are defined same as u, f and g. Also, physical Interpretation of Solving the Eikonal Equation: In a homogeneous medium the characteristic curves are straight lines (light rays) and an initial planar wavefront propagates in the direction orthogonal to them. So, all wavefronts are planar or we can say a surface of a fixed optical phase while the wavefronts propagate orthogonally to the (light rays) [2,36]. Moreover, here are some important sources related to recent developments in this topic [28,31–34,48].

* Corresponding author.
E-mail address: rostamy@khayam.ut.ac.ir (D. Rostamy).
Peer review under responsibility of Faculty of Engineering, Alexandria University.

https://doi.org/10.1016/j.aej.2021.10.003
1110-0168 © 2021 THE AUTHORS. Published by Elsevier BV on behalf of Faculty of Engineering, Alexandria University.
This is an open access article under the CC BY-NC-ND license (http://creativecommons.org/licenses/by-nc-nd/4.0/).

In Eq. (1) $u(x,y)$ represents the wave propagation time and $f(x,y)$ represents the wave propagation velocity. There are many analytical methods for such physical problems, but using them is not an easy task or it is not possible to solve them. Therefore, we need appropriate numerical methods with high accuracy. That is why scientists decided to explore a suitable and compatible way to improve the approximate solution of the Eikonal equation. There are various numerical methods for calculating nonlinear differential equations, some of which may be more costly in terms of numerical calculations. So, for numerical computations, convergence speed, response accuracy and error reduction are the main phenomena of numerical algorithms. A fast sweeping method for numerical solution of Eikonal equations in a (rectangular grid) is presented and Gauss–Seidel iterations are used [51]and a new sweeping algorithm using an explicit formula, efficiency, accuracy is discussed with numerical examples in two and three dimensions [21]. Stability of the maximal solution to the geometric Eikonal equation and their existence has been investigated in [7]. The travel time error due to the solution of the Eikonal equation based on the finite difference is investigated using the fast sweeping method (FSM) to solve the factored Eikonal equation [15]. The Eikonal equation can also be considered as a short-wavelength range of the geometric wave equation. As you know, sound waves and elastic waves are still important physical phenomena. Such as (electromagnetic waves and water waves controlled by wave propagation) and wave propagation in a moving fluid [27]. Existence theorems, uniqueness theorems and stability theorems for the viscosity solutions of the Hamilton–Jacobi equation [6] and For the RBF solution of the Eikonal equation has been investigated using the boundary knot method and the analog equation method in [9]. The operator-splitting based fast sweeping methods have been developed to solve an anisotropic Eikonal equation induced by isotropic wave propagation in a moving fluid [12]. The Eikonal equation is proposed by the fast sweep method in rectangular grids to improve the speed of the method in general and in particular in cases where the speed is changing rapidly [3]. One of the important applications of Eikonal equation is imaging and travel time tomography, so the calculation of travel time for (travel time isotropic) media based on an ellipticity parameter perturbation for the discretized of Eikonal equation (transversely isotropic) has been obtained using the fast sweep [17,39] and For irregular topographies, the solution of time-dependent Hamilton–Jacobi equations with a point-source condition by the RKDG method has been extensively investigated in [22]. Numerical solution of Eikonal Equation for large Number of waves Chebyshev Pseudospectral viscosity method has been used [30]. The original Eikonal equation has been computed during the Gauss- Seidel iterations, and the use of the fast sweeping method for (factored Eikonal equation) has been developed [55]. The fast-marching method for the generalized (anisotropic) Eikonal equation for wavefront propagation called the characteristic fast marching method has been developed, also new algorithm has been proposed [14] and the electromagnetic theory of propagation has been investigated in [18].

Recent developments show that the Eikonal equation is one of the partial differential equations that is widely used in science, so it has attracted the attention of researchers and has increased significantly in recent years. Researchers have proposed various numerical solutions and algorithms for Eikonal equation problems. The Researchers described the use of the Eikonal equation instead of the complete Helmoltz equation in [25]. They have analyzed the errors due to neglect of the wave field in Eikonal tomography and investigated the phase-velocity errors using a Gaussian filter. Therefore, phase-velocity maps of the gradient of these travel time fields can be obtained by Eikonal Equation [24]. The use of the Eikonal equation to simulate the heart valve by algorithms based on standard finite element methods has been extensively investigated [13]. Researchers have developed a new sixth-order nonlinear acoustic Eikonal equation that results in one Real, Two-complex conjugate solution [50]. The fast sweeping method for anisotropic Eikonal equations with finite difference approximation using Gauss–Seidel iterations [16] and the improved FS method with an upwind finite difference scheme for solving the Eikonal equation are presented [8]. The upwind scheme has been used to discretize the Eikonal equation [41]. For inference (three-dimensional surface of shading image) Shape-from-shading method using fast Eikonal solvers has been investigated [49].

In this research, we study a comprehensive investigate on the DQ method [52,43] for numerical solutions of the Eikonal equation. The DQ method is an excellent method that has higher convergence speed than the existing methods. This method has high accuracy and low computational volume. This can be achieved in a very short time by the DQ method of solving the Eikonal equation compared to the existing methods. We try to reduce the errors and obtain the convergence with high velocity. For the purposes of this paper, we are developing a new grid-point scheme [45], which is very effective in numerical solution of the Eikonal equation and error reduction. In DQ method the derivative is approximated by a variable with the weighted coefficients at all discrete points, so it is not dependent on the grid points and the derivative. We consider two methods polynomial differential quadrature (PDQ) and fourier differential quadrature (FDQ) [53] here for the solution of Eq. (1). Both methods are useful for solving the Eikonal equation, but the PDQ method for solving the Eikonal equation is more accurate. For both methods we have tested the NGP and obtained good results for Problem (1). There are many articles that have used numerical methods such as fast sweeping and fast Marching to solve the Eikonal equation and developed [54,51,21,15,27,3]. So far, no research has been done on the use of the DQ method to solve the Eikonal equation.

The DQ method is one of the most powerful and effective methods for solving nonlinear partial differential equations with high accuracy [29]. The DQ method has been implemented by researchers in various fields and has attempted to develop it using different interpolations, polynomials, splines, radial base function, to better respond. The DQ method was used by G-spline interpolation for the thin plate problem has been studied in [29] and an effective DQM which is based on modified cubic B-spline has been implemented for the nonlinear Schrödinger (NLS) equation in [4]. Harmonic DQ method for vibration equation has been studied in [42].

The outline of this paper is as follows. In Section 2, we discuss the DQ method [47] on the two-dimensional problem. The PDQ and FDQ methods and weighting coefficients are introduced by Lagrange interpolation in this section. The weighting coefficients for the first-order derivatives and the weighting coefficients for the second-order derivatives are presented in

this part for PDQ and FDQ methods. In Section 3, the new grid points (NGP) are introduced, which have excellent accuracy and convergence speed. Then the selection of grid points in accuracy and convergence speed plays an important role. In Section 4, we adapt the new implementation of the FDQ and PDQ methods [53] to the 2D and 3D dimensional Eikonal equation based on NGP. To solve the numerical problem, we have discrete the Ekanol equation. In Section 5, the numerical results are computed based on the FDQ and PDQ methods using the L_1, L_∞ error norm [4,19]. We have compared the errors of various two and three-dimensional problems and their results are abridged in Section 6.

2. Review of DQ method

First we review DQ method that it is one of the numerical methods that is widely used in different parts of ordinary differential equations and some partial differential equations [52,43]. Then, we use the improvement of DQ method for solving the Eikonal equation. One of the features of this method is that it requires fewer grid points in numerical calculations than some existing methods. This method was first proposed by Bellman [5], later developed by Shu and Richards [46,47]. We introduce the approximate derivatives the first-order for a 2-D problem in the domain $a \leqslant x \leqslant b, a \leqslant y \leqslant b$ are given by:

$$u_x^{(1)}(x_i, y_j) = \sum_{k=1}^{N_x} a_{ik}^x u(x_k, y_j), \qquad i = 1, 2, \ldots, N_x \tag{2}$$

and

$$u_y^{(1)}(x_i, y_j) = \sum_{k=1}^{N_y} a_{jk}^y u(x_i, y_k), \qquad j = 1, 2, \ldots, N_y. \tag{3}$$

Where $u_x^{(1)}, u_y^{(1)}$ are the approximate derivatives of the first order in the points (x_i, y_j) in the direction of x, y and u at the ij^{th} point. Also, we assume that a_{ik}^x and a_{jk}^y the weighting coefficients in the x and y directions. Morover, N_x and N_y are the number of grid points in the x and y directions in the domain. Similarly, the approximate second-order derivatives are as follows:

$$\frac{\partial^2 u(x_i, y_j)}{\partial x^2} = \sum_{k=1}^{N_x} b_{ik} u(x_k, y_j), \tag{4}$$

$$\frac{\partial^2 u(x_i, y_j)}{\partial y^2} = \sum_{k=1}^{N_y} b_{jk} u(x_i, y_k) \tag{5}$$

and

$$\frac{\partial^2 u(x_i, y_j)}{\partial x \partial y} = \sum_{l=1}^{N_x} a_{il} \sum_{k=1}^{N_y} a_{jk} u(x_l, y_k). \tag{6}$$

Where b_{ik} and b_{jk} are the DQ weighting coefficients [26]. Similarly, for the 3D differential equation, all derivatives are approximated in their respective direction and the functional value at all grid points, for n^{th} order derivatives of u. We write

$$\left.\frac{\partial^n u}{\partial x^n}\right|_{x=x_i} = \sum_{j=1}^{N} w_{ij}^{(n)} u_j, \qquad i = 1, 2, \ldots, N. \tag{7}$$

Where $w_{ij}^{(n)}$ are the weighting coefficients of the nth order derivative of (x_i, y_i).

2.1. PDQ method

In the PDQ method, the Lagrange interpolation polynomials are used. The explicit formulas for the calculation of weighted coefficients have been substantiated by Quan and Chang basic Lagrange interpolation. Later generalized by Shu and Richards [45]. If $a_k, k = 1, 2, \ldots, N$, where the $S^{(1)}(x)$ is the first derivative of $S(x)$ [52,43,44]. We know that the Lagrange interpolation polynomials are as follows:

$$a_k(x) = \frac{S(x)}{(x - x_k) S^{(1)}(x_k)}. \tag{8}$$

Where, we consider

$$\begin{cases} S(x) = \prod_{j=1}^{N} (x - x_j), \\ S^{(1)}(x_k) = \prod_{\substack{j=1 \\ j \neq k}}^{N} (x_k - x_j). \end{cases} \tag{9}$$

Now from (8), we find the weighted coefficients for the first - order derivatives

$$\begin{cases} a_{ij} = \frac{S^{(1)}(x_j)}{(x_i - x_j) S^{(1)}(x_j)} & for \quad j \neq i, \quad i, j = 1, 2, \ldots, N, \\ a_{ii} = -\sum_{\substack{j=1 \\ i \neq j}}^{N} a_{ij}, & i = 1, 2, \ldots, N \end{cases} \tag{10}$$

where the weighted coefficients of the second-order derivative is as follows

$$\begin{cases} b_{ij} = 2a_{ij}\left[a_{ii} - \frac{1}{x_i - x_j}\right] & for \quad j \neq i, \quad i, j = 1, 2, \ldots, N, \\ b_{ii} = -\sum_{\substack{j=1 \\ i \neq j}}^{N} b_{ij}, & i = 1, 2, \ldots, N. \end{cases} \tag{11}$$

Also, $x_i, i = 1, 2, \ldots, N$, are the grid points that we choose arbitrarily. Similarly, for high-order derivatives in [44] it is suggested.

2.2. FDQ method

Here we consider the Fourier series expansion as follows:

$$f(x) = b_0 + \sum_{k=1}^{N/2} (c_k \cos \omega + d_k \sin \omega). \tag{12}$$

Therefore, we approximate the function with the Fourier series such that $f(x)$ is defined and single-valued except possibly at a finite number of points in $(|L, L), f(x)$ is periodic outside $(|L, L)$ with period $2L$ and $f(x)$, $f'(x)$ are piecewise continuous in $(|L, L)$ for $\omega = \frac{k\pi x}{L}$. We use the Lagrange interpolated trigonometric polynomials for the FDQ approach, [52,43,10,44]. The weighted coefficients a_{ij}, b_{ij} for the first-order and second-order derivatives are as follows:

$$\begin{cases} a_{ij} = \frac{1}{2}\cdot\frac{p(x_i)}{\left[\sin\frac{(x_i-x_j)}{2}\right]p(x_j)} & for \quad j\neq i, \quad i,j=1,2,\ldots,N, \\ a_{ii} = -\sum\limits_{\substack{j=1\\ i\neq j}}^{N} a_{ij}. \end{cases} \tag{13}$$

$$\begin{cases} b_{ij} = a_{ij}\left[2a_{ii} - \cot\frac{x_i-x_j}{2}\right] & for \quad j\neq i, \quad i,j=1,2,\ldots,N. \\ b_{ii} = -\sum\limits_{\substack{j=1\\ i\neq j}}^{N} b_{ij}. \end{cases} \tag{14}$$

Where

$$p(x_i) = \prod_{\substack{j=0\\ i\neq j}}^{N} \sin\frac{(x_i - x_j)}{2}. \tag{15}$$

3. Generation of new grid points

The DQ method has shown that non-uniform of grid points yields best consequence than grid points of equal distance. The five types of grid points usually used in most articles are compared in [45]. The Chebyshev-Gauss–Lobatto points (CGLP), which are commonly found in most articles, such as:

$$x_i = \frac{1}{2}\left(1 - \cos\left(\frac{i-1}{N-1}\pi\right)\right), \qquad i = 1,2,\ldots,N. \tag{16}$$

The Chebyshev-Gauss–Lobatto distribution also has been used in [46,47,10]. Here, we define the novel grid points (NGP). We are inspired by the difference between the two Chebyshev-Gauss–Lobatto distributions in [26], such that we define:

$$x_i = a + \frac{(b-a)}{2}\left(\frac{\cos\left[\frac{(i-1)\pi}{N-1}\right]}{\cos\left[\frac{\pi}{2N}\right]} + 1 - \frac{\cos\left[\frac{(2i-3)\pi}{2(N-1)}\right]}{\cos\left[\frac{\pi}{2(N-1)}\right]} + 1\right)$$
$$i = 1,2,\ldots,N. \tag{17}$$

The motivations of the choice and arrangement of NGP are based on experimental results of norm for residual (or error) and stability. Also, we remark in non-uniform distribution (17), N represents the number of grid points in each direction for a domain $[a,b]$. We observe that in the next section the distribution (17) is useful for high accuracy.

4. PDQ and FDQ Methods for solving (1)

In this section, we scrutinize the implementation of the methods PDQ and FDQ by NGP. We claim that these methods have converges rapidly in different examples. Now, we presume that the calculating domain is $[a,b]$. Using (1) (in case 2D), (2) and (3), we have:

$$\left(\sum_{k=1}^{N_x} a_{i,k}u_{k,j}\right)^2 + \left(\sum_{k=1}^{N_y} \overline{a}_{j,k}u_{i,k}\right)^2 = f^2(x_i,y_j) \tag{18}$$

where, $a_{i,k}$ and $\overline{a}_{j,k}$ are the weighted coefficients of the first-order derivative of u with respect to x and y respectively and $f_{i,j}$ is a given function. Similarly, by using (1) (in case 3D), (2) and (3), we have:

$$\left(\sum_{k=1}^{N_x} a_{i,k}u_{k,j,\kappa}\right)^2 + \left(\sum_{k=1}^{N_y} \overline{a}_{j,k}u_{i,k,\kappa}\right)^2 + \left(\sum_{k=1}^{N_z} \tilde{a}_{\kappa,k}u_{i,j,\kappa}\right)^2 = f^2(x_i,y_j,z_\kappa) \tag{19}$$

where $a_{i,k}, \overline{a}_{j,k}, \tilde{a}_{\kappa,k}$ the weighted coefficients of the first-order derivative of u with respect to x, y and z respectively.

To use the PDQ method, $a_{i,k}, \overline{a}_{j,k}, \tilde{a}_{\kappa,k}$ weighted coefficients are calculated by Eq. (10). For the FDQ method, the weight coefficients $a_{i,k}, \overline{a}_{j,k}, \tilde{a}_{\kappa,k}$ are calculated by Eq. (13) and (15).

N_x, N_y and N_z are the number of grid points in the x, y and z directions at the domain. We use (18) for the two dimensional Eikonal equation and we apply (19) for the three-dimensional equation. We propose the following algorithm for solving (1).

4.1. Algorithm of PDQ or FDQ at NGP or CGLP

- **Step 1**- N, ϵ and the weight coefficients are given i.e (13) and (15).
- **Step 2**- From method of PDQ (or FDQ) at NGP or CGLP we obtain a nonlinear system i.e. (18) (or (19))
- **Step 3**- We obtain an initial guess by gradient descent method with an initial point same as zero.
- **Step 4**- Broyden-Fletcher-Goldfarb-Shanno (BFGS) algorithm is used for iterative the sequens of solutions by initial guess of step3.
- **Step 5**- Convergence can be checked by observing the norm of the gradient $\leqslant \epsilon$.

Remark 1. In the above algorithm, we assume that N is the number of mesh points and the number of iterations is shown by M which it is dependent on ϵ. We remark that the solution to the Eikonal equation is not necessarily differentiable. In this case study, the methods designed for fast computation of smooth solutions are suitable. Therefore, for non-smooth solutions, We need to an improvement scheme.

5. Numerical results

According to the purposes of this article, we investigate the approximated solution of the Eikonal equation using the PDQ and FDQ as numerical methods at NGP or CGLP. The accuracy and effectiveness of our numerical methods are illustrated by numerical examples. The following error are defined by L_1 and L_∞ norms:

$$E_N^{(L_1)} = \sum_{i,j=1}^{N}\left|u_{i,j}^{(exact)} - u_{i,j}^{(app)}\right|, \tag{20}$$

$$E_N^{(L_\infty)} = \max_{i,j=1}^{N}\left|u_{i,j}^{(exact)} - u_{i,j}^{(app)}\right| \tag{21}$$

and

$$ratio = \frac{E_{N-1}^{(k)}}{E_N^{(k)}}, \qquad k = L_1, L_\infty \tag{22}$$

where $u_{i,j}^{(exact)}$ and $u_{i,j}^{(app)}$ denote the exact solution and approximated solution respectively.

Remark 2. The convergence rates for the iterative processes are investigated by quantify of ratio because we have not any estimated theoretically. Also, we consider $\epsilon = 10^{-5}$ or $M = 100$

(number of iterations) as stopping criterion in all of examples. Hence, we observe that in following example iterations in Figs. 2, ...,9 are converge and rate of convergence is dependent on ratio (see Tables 1–5).

Remark 3. For investigating of stability of methods, we know that a small perturbation in initial data may generate a large amount of perturbations in the solution. Therefore, we apply noisy data to show the stability of the proposed methods:

$$\tilde{a}_{i,j} = a_{i,j}(1 + \epsilon.rand(ij)), \quad i,j = 1, ..., N.$$

where $a_{i,j}$ is the exact data and $rand(ij)$ is a random number with uniform distribution of the interval $[-1, 1]$. The magnitude ϵ displays the noise level of the measurement data.

Remark 4. The following examples are not artificial and are motivated by the following applications:

- Example 1. This arises from optical instruments and components [44,1].
- Example 2. This example occurs from optics and laser technology aims to provide a vehicle [23,20].
- Example 3. This problem gets up in quantum field theory [11,1].
- Example 4. This example happens for the screened coulomb potential [20].
- Example 5. This example arises in quantum mechanics [11,1].

Example 1. We consider 2-D Eikonal equation. The domain is $\Omega = [-1, 1] \times [-1, 1]$ with the function

$$f(x, y) = \frac{\pi}{2}\sqrt{\sin^2\left(\pi + \frac{\pi}{2}x\right) + \sin^2\left(\pi + \frac{\pi}{2}y\right)}.$$

Where Γ is the points $\Gamma = \left\{\left(\frac{1}{4}, \frac{1}{4}\right), \left(\frac{3}{4}, \frac{3}{4}\right), \left(\frac{1}{2}, \frac{1}{2}\right), \left(\frac{1}{2}, -\frac{1}{2}\right), (0, 0)\right\}$ and $g\left(\frac{1}{4}, \frac{1}{4}\right) \approx -1.848$, $g\left(\frac{3}{4}, \frac{3}{4}\right) \approx -0.765$, $g\left(\frac{1}{2}, \frac{1}{2}\right) = g\left(\frac{1}{2}, -\frac{1}{2}\right) = -\sqrt{2}$ and $g(0, 0) = -2$. The true solution for the Eikonal equation is $u(x, y) = \cos\left(\pi + \frac{\pi}{2}x\right) + \cos\left(\pi + \frac{\pi}{2}y\right)$. We now use both FDQ and PDQ methods to solve the Eikonal equation. The three-dimensional and two-dimensional contour plot is shown in Fig. 1. The L_∞ error is shown in Table 1 and we also present the error plot of L_∞ in Fig. 2.

Table 1 Errors and the convergence ratio in the L_∞, for Example 1.

	FDQ				*PDQ*			
	CGLP		*NGP*		*CGLP*		*NGP*	
N	L_∞	Ratio	L_∞	Ratio	L_∞	Ratio	L_∞	Ratio
5	$4.51E-2$		$1.55E-2$		$7.03E-2$		$1.55E-2$	
7	$9.80E-3$	4.6	$1.86E-2$	0.8	$2.34E-2$	1	$1.86E-2$	0.8
17	$2.08E-3$	4.7	$2.09E-9$	8.9	$2.73E-4$	86	$2.09E-9$	8.9
21	$1.83E-3$	1.1	$5.20E-11$	40.1	$4.24E-5$	6.4	$5.20E-11$	40.1

Table 2 Comparing Errors Accuracy in the L_1 , L_∞ norms for Example 2.

	FDQ				*PDQ*			
N	L_1	Ratio	L_∞	Ratio	L_1	Ratio	L_∞	Ratio
13	$2.54E-2$		$3.21E-4$		$4.07E-5$		$4.42E-7$	
15	$5.67E-3$	4.5	$5.37E-5$	6	$1.68E-6$	24.3	$1.31E-8$	33.8
21	$5.48E-5$	103.4	$2.87E-7$	187.9	$5.11E-11$	32809.5	$2.31E-13$	56438.9
25	$2.33E-6$	23.5	$9.31E-9$	30.8	$6.18E-12$	8.3	$2.40E-14$	9.7

Table 3 The L_∞, errors and their convergence ratios, for Example 3.

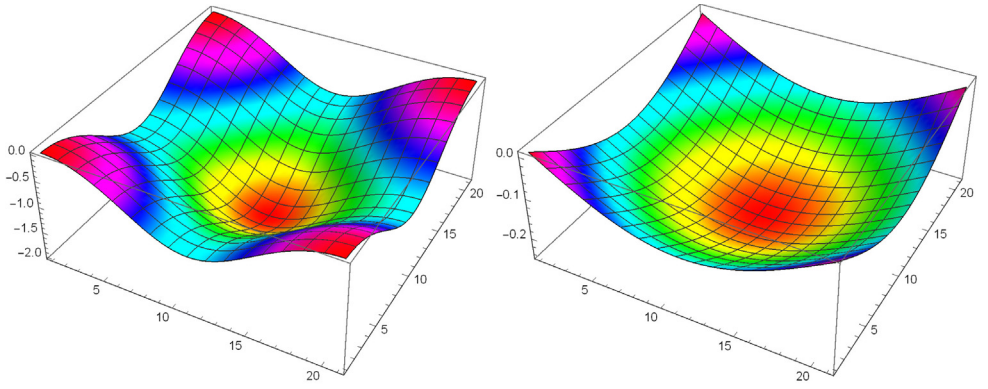
	FDQ				*PDQ*			
	CGLP		*NGP*		*CGLP*		*NGP*	
N	L_∞	Ratio	L_∞	Ratio	L_∞	Ratio	L_∞	Ratio
4	$2.84E-1$		$6.50E-2$		$8.83E-1$		$9.87E-3$	
6	$1.16E-1$	2.4	$8.52E-3$	2.9	$4.12E-2$	21.5	$3.03E-4$	5.0
8	$8.20E-2$	1.4	$2.47E-5$	8.4	$3.36E-4$	122.4	$7.68E-9$	15.2
10	$1.99E-2$	4.2	$4.65E-11$	19.0	$1.51E-6$	222.3	$2.53E-11$	8.2

Table 4 Comparing Errors Accuracy in the L_1 , L_∞ norms for Example 4.

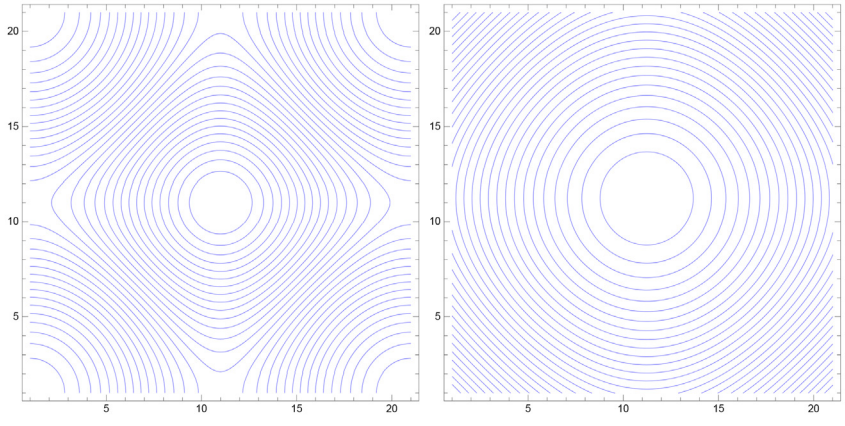
		FDQ				*PDQ*		
N	L_1	Ratio	L_∞	Ratio	L_1	Ratio	L_∞	Ratio
9	$4.71E-4$		$2.19E-5$		$1.22E-6$		$6.61E-8$	
13	$1.93E-5$	24.4	$4.42E-7$	49.5	$1.25E-9$	974.5	$3.47E-11$	1904.9
15	$3.87E-6$	5	$6.80E-8$	6.5	$3.83E-11$	32.8	$8.19E-13$	42.4
17	$7.74E-7$	5	$1.08E-8$	6.3	$1.21E-12$	31.7	$2.10E-14$	39.3
19	$1.54E-7$	5	$1.76E-9$	6.2	$1.11E-13$	10.9	$1.11E-15$	18.8

Table 5 Comparing Errors Accuracy in the L_1 , L_∞ norms for Example 5.

		FDQ				*PDQ*		
N	L_1	Ratio	L_∞	Ratio	L_1	Ratio	L_∞	Ratio
12	$2.40E-1$		$1.36E-2$		$7.37E-2$		$1.11E-3$	
15	$9.54E-4$	252.	$2.39E-5$	569.5	$1.04E-5$	7107.1	$2.70E-7$	4112.7
25	$3.96E-5$	24.15	$1.30E-6$	18.4	$1.18E-9$	8826.7	$1.20E-11$	22510.
40	$1.03E-6$	38.5	$8.72E-9$	149.5	$1.80E-13$	6542.7	$2.18E-15$	5508.3

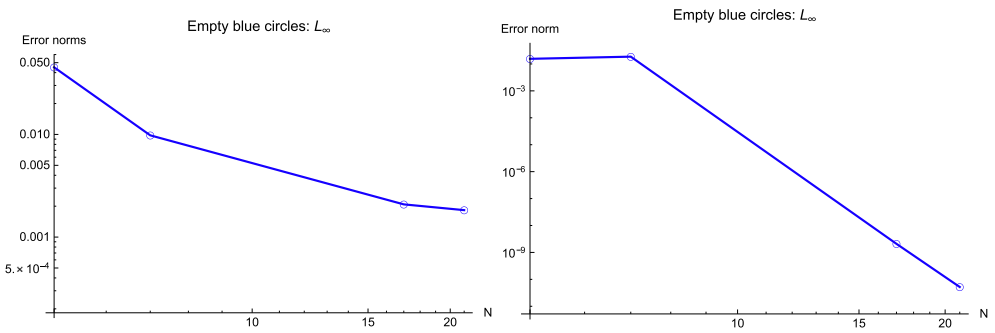


(a) 3-D contour plot numerical solution with CGLP (b) 3-D contour plot numerical solution with NGP

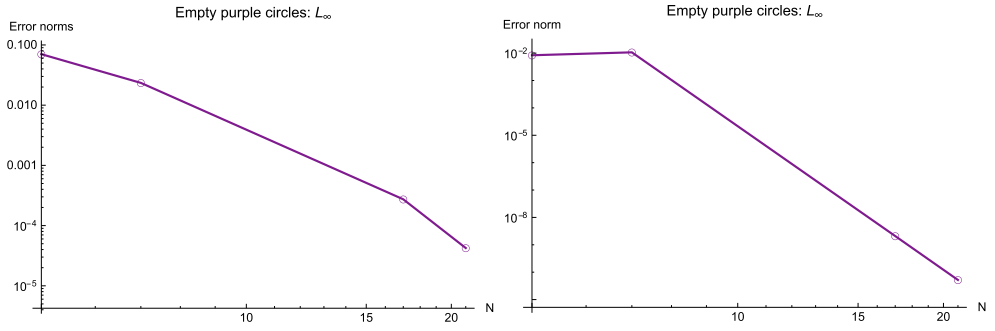


(c) Contour plot numerical solution with CGLP (d) 2-D Contour plot of the solution with NGP

Fig. 1 Figures (a) and (c) show the numerical solution of the Eikonal equation using CGLP. Also, figures (b) and (d) present the numerical solution of the Eikonal equation using from the NGP for Example 1.



(a) The error for the FDQ method with CGLP (b) The error for the FDQ method with NGP



(c) The error for the PDQ method with CGLP (d) The error for the PDQ method with NGP

Fig. 2 Comparison of errors in FDQ and PDQ methods. We have shown the empty blue circles L_∞ for FDQ and the empty purple circles L_∞ Errors for PDQ method. We used the Chebyshev grid points for (a), (c) and the new grid points for (b), (d) in Example 1.

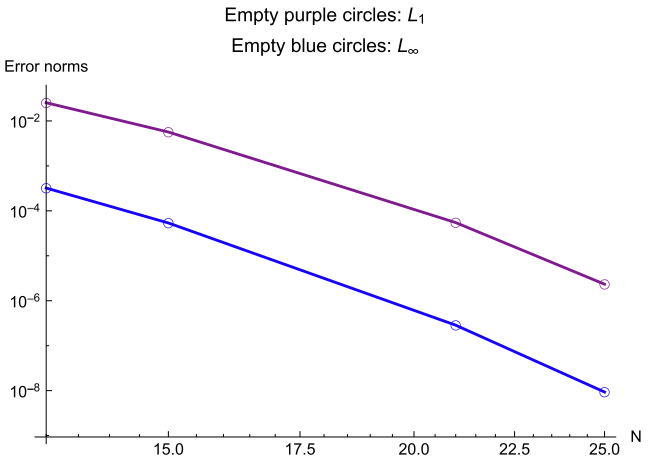


Fig. 3 The Accuracy of FDQ method error norms (We used empty purple circles L_1 and the empty blue circles L_∞) for Example 2.

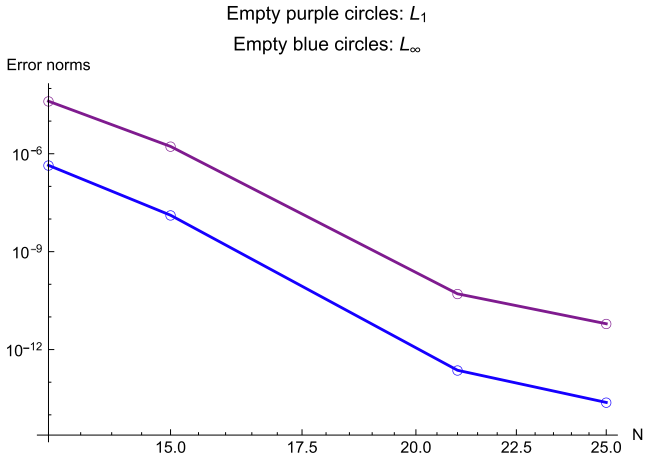


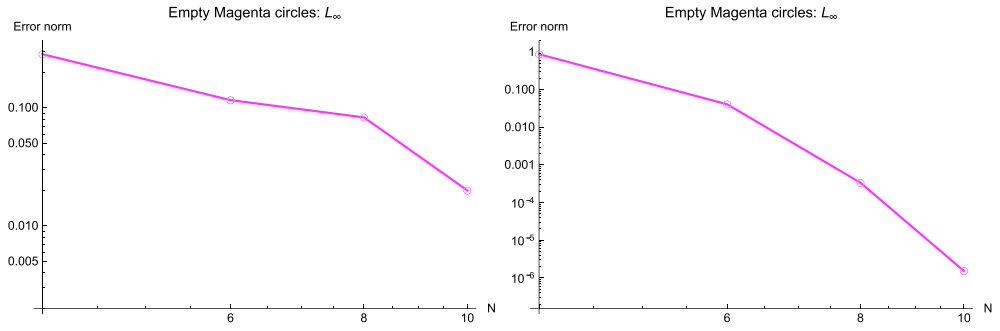
Fig. 4 The Accuracy of PDQ method error norms (We used empty purple circles L_1 and the empty blue circles L_∞) for Example 2.

Example 2. Consider Eq. (1) with $\Omega = [-1,1]\times[-1,1]$ and Γ is the point $(0,0)$. The exact solution of the Ekional equation is $u(x,y) = e^{x^2+y^2}$ with $f(x,y) = 2e^{(x^2+y^2)}(x^2+y^2)^{\frac{1}{2}}$. Now we implement FDQ and PDQ methods, and we use the CGLP. To measure the accuracy of this example, the error norms L_1, L_∞ With The Convergence ratio are shown in Table 2. The error norms plots are shown in Figs. 3 and 4.

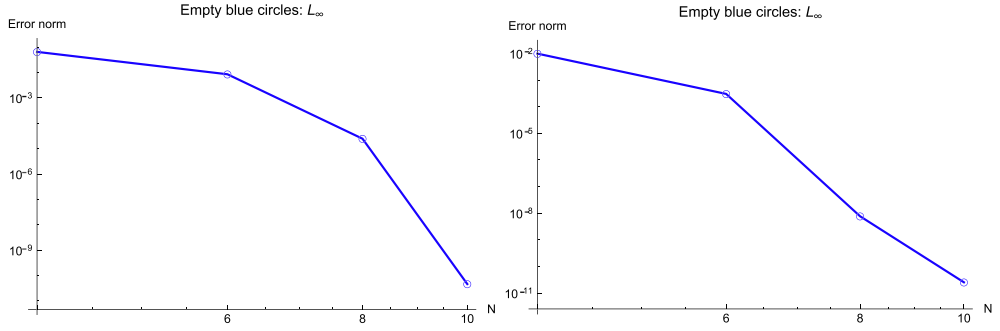
Example 3. We consider 3-D Eikonal equation with $\Omega = [-1,1]\times[-1,1]\times[-1,1]$. and $\Gamma = \{(0,0,0)\}$. The exact solution of the Eikonal equation for this problem is

$$u(x,y,z) = \cos(x) + \cos(y) + \cos(z).$$

We implement FDQ and PDQ methods using the CGLP and the NGP distribution. The L_∞ error is presented in Table 3.



(a) The error for the FDQ method using CGLP (b) The error for the PDQ method using CGLP



(c) The error in the FDQ method using NGP (d) The error in the PDQ method using NGP

Fig. 5 Comparison of errors in FDQ and PDQ methods (we used empty Magenta circles L_∞, using the CGLP and the empty blue circles L_∞ using the NGP). We used the Chebyshev grid points for (a), (b) and the new grid points for (c), (d) for Example 3.

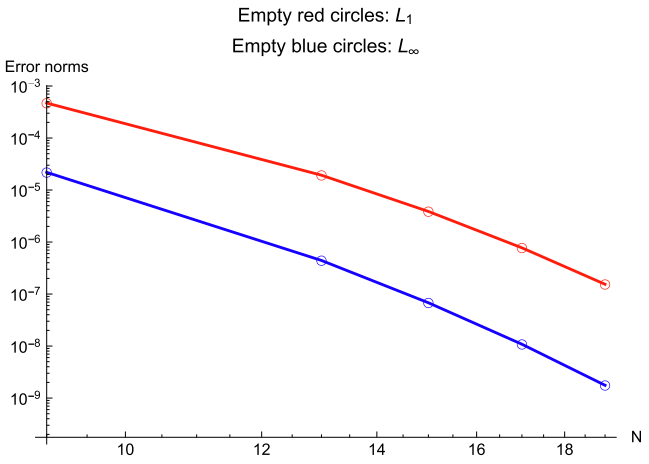


Fig. 6 The Accuracy of FDQ method error norms (We used empty red circles L_1 and the empty blue circles L_∞) for Example 4.

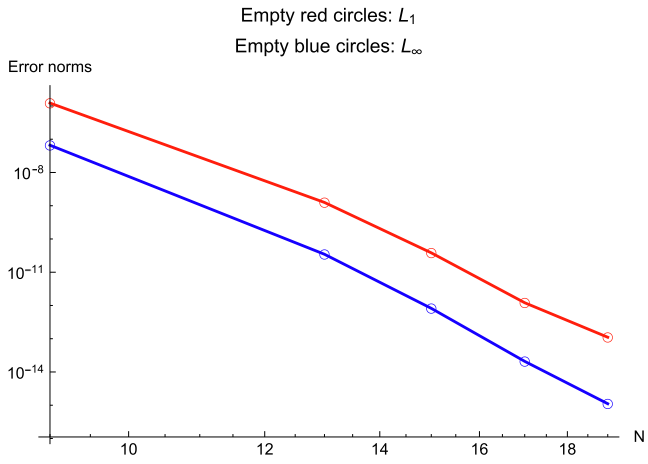


Fig. 7 The Accuracy of PDQ method error norms (We used empty red circles L_1 and the empty blue circles L_∞) for Example 4.

In this example, due to the effectiveness of the error reduction scheme, we have shown the contour plot of the numerical solution in three dimensions using a CGLP and the NGP in Fig. 10. Where the error plots shown in Fig. 5. The function f is given, such as,

$$f(x,y,z) = \left(\sin^2(x) + \sin^2(y) + \sin^2(z)\right)^{\frac{1}{2}}.$$

Example 4. Consider Eq. (1) with $\Omega = [-1,1] \times [-1,1]$ and Γ is the point $(0,0)$ In this example we use CGLP for both methods. The error plot is shown in Figs. 6 and 7. The exact solution of the Eikonal equation is

$$u(x,y) = \frac{5}{(9 + x^2 + y^2)^{\frac{1}{2}}}.$$

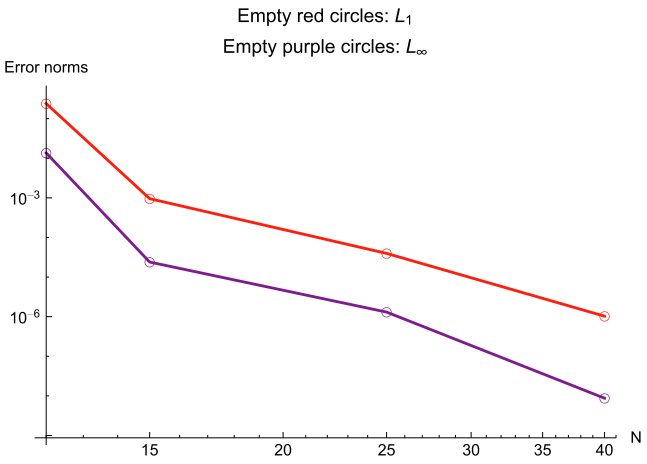


Fig. 8 The Accuracy of FDQ method error norms (We used empty red circles L_1 and the empty purple circles L_∞) for Example 5.

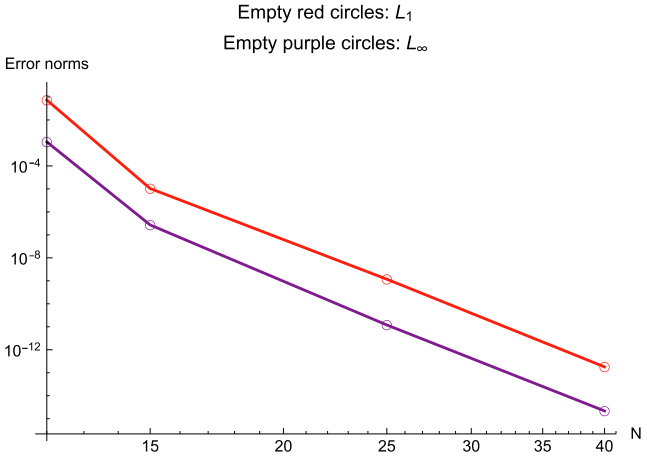


Fig. 9 The Accuracy of PDQ method error norms (We used empty red circles L_1 and the empty purple circles L_∞) for Example 5.

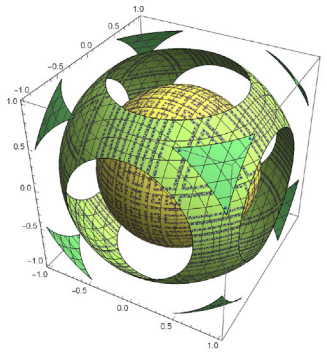
To measure the accuracy of this example, the error norms L_1, L_∞ and The Convergence ratio is shown in Table 4. Where the function $f(x, y)$ is given, such as,

$$f(x,y) = 3\left(\frac{x^2+y^2}{(9+x^2+y^2)^3}\right)^{\frac{1}{2}}.$$

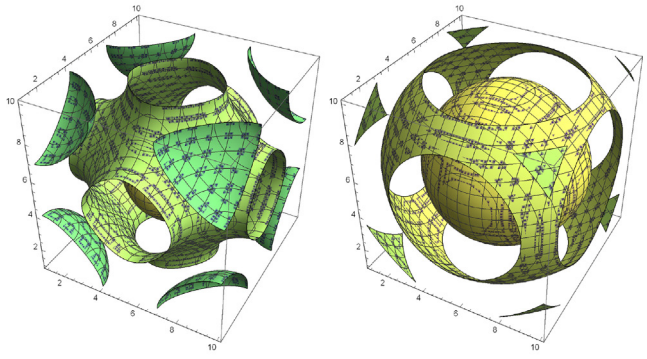
Example 5. The 2-D Eikonal equation for problem (1). The computational domain is $\Omega = \left[-\frac{1}{\sqrt{\pi}}, \frac{1}{\sqrt{\pi}}\right] \times \left[-\frac{1}{\sqrt{\pi}}, \frac{1}{\sqrt{\pi}}\right]$ and Γ is the point $(0, 0)$ with the exact solution as

$$u(x,y) = cos(2\pi x)cos(2\pi y).$$

In this example, we study both methods FQD and PDQ and for this case used the CGLP. To compare the measurement of the research, approach, the L_1, L_∞ errors presented in Table 5. The error plots are shown in Figs. 8 and 9. Here we consider



(a) Contour plot of the exact Solution



(b) Numerical Solution using CGLP (c) Numerical Solution using NGP

Fig. 10 Comparison of exact Solution versus the numerical Solution: (a) The 3-D Contour plot of the exact Solution $u(x, y, z)$, (b) is the 3-D contour plot of numerical Solution $u(x, y, z)$ using CGLP and (c) is the 3-D contour plot of numerical Solution $u(x, y, z)$ using NGP, for Example 3.

$$f(x,y) = \pi\sqrt{2 - 2\cos(4\pi x)\cos(4\pi y)}.$$

6. Conclusion and future recommendations

In this paper, we presented a new grid point's scheme (NGP) to solve Eikonal equations to reduce the error and ratio of convergence speed. The algorithms of PDQ and FDQ proposed in the current paper was tested on several examples. We observe that the PDQ and FDQ schemes using NGP are the best approach to Eikonal equation. One of the achievements of this study is development of DQ methods for these equations. The obtained results of the PDQ at NGP demonstrate reliability and efficiency of the scheme. Another considerable advantage of the proposed schemes is that they require less complicated computation of operations to obtain approximate solution. Moreover, we investigated the stability of the schemes by a small perturbation in initial data. On the other hand, we know that the solution to the Eikonal equation is not necessarily differentiable. In this paper, methods designed for fast computation of smooth solutions are not studied. The authors plan to study this important problem in the future by improve the DQ methods for this problem. Another topic that can be expanded in this area is the study of coupling issues of Eikonal equations

that we will address in the future. Also, we need to change different strategies of family of DQ for solving some well-posed and ill-posed problems with higher order derivatives. Due to the high volume of new content of this paper, we postpone it to future works. On the other hands, our goal in the future is to produce methods based on new methods of finite elements [35,37,38,40] and combining them with the methods described in this article, which will increase accuracy and efficiency.

Declaration of Competing Interest

The authors declare that they have no known competing financial interests or personal relationships that could have appeared to influence the work reported in this paper.

Acknowledgements

The authors would like to thank the referees for some comments which have led to an improvement of the paper.

References

[1] S. Abdu, Computation of the total scattering cross sections for the halogens, Science World Journal 13 (4) (2018) 35–38.
[2] E. Arshid, A.R. Khorshidvand, Free vibration analysis of saturated porous fg circular plates integrated with piezoelectric actuators via differential quadrature method, Thin-Walled Structures 125 (2018) 220–233.
[3] S. Bak, J. McLaughlin, D. Renzi, Some improvements for the fast sweeping method, SIAM Journal on Scientific Computing 32 (5) (2010) 2853–2874.
[4] A. Bashan, N.M. Yagmurlu, Y. Ucar, A. Esen, An effective approach to numerical soliton solutions for the schrödinger equation via modified cubic b-spline differential quadrature method, Chaos, Solitons & Fractals 100 (2017) 45–56.
[5] R. Bellman, B. Kashef, J. Casti, Differential quadrature: a technique for the rapid solution of nonlinear partial differential equations, Journal of computational physics 10 (1) (1972) 40–52.
[6] M.G. Crandall, P.L. Lions, Viscosity solutions of hamilton-jacobi equations, Transactions of the American mathematical society 277 (1) (1983) 1–42.
[7] J. Cruz-Sampedro, E. Skibsted, Global solutions to the eikonal equation, Journal of Differential Equations 255 (12) (2013) 4337–4377.
[8] D. Cui, Y. Zhang, C. Wang, N. Qin, Y. Hu, Q. Zeng, Z. Zhang, A hybrid-order strategy to accelerate a high-order fast sweep method, J. Geophys. Eng. 17 (4) (2020) 661–669.
[9] M. Dehghan, R. Salehi, A boundary-only meshless method for numerical solution of the eikonal equation, Comput. Mech. 47 (3) (2011) 283–294.
[10] H. Ersoy, K. Mercan, Ö. Civalek, Frequencies of fgm shells and annular plates by the methods of discrete singular convolution and differential quadrature methods, Compos. Struct. 183 (2018) 7–20.
[11] M.A. García-Sánchez, F. Rojas-González, E.C. Menchaca-Campos, S.R. Tello-Solís, R. Quiroz-Segoviano, L.A. Diaz-Alejo, E. Salas-Bañales, A. Campero, Crossed and linked histories of tetrapyrrolic macrocycles and their use for engineering pores within sol-gel matrices, Molecules 18 (1) (2013) 588–653.
[12] R. Glowinski, S. Leung, J. Qian, Operator-splitting based fast sweeping methods for isotropic wave propagation in a moving fluid, SIAM Journal on Scientific Computing 38 (2) (2016) A1195–A1223.
[13] J. Hiromi Spühler, J. Hoffman, An interface-tracking unified continuum model for fluid-structure interaction with topology change and full-friction contact with application to aortic valves, Int. J. Numer. Meth. Eng. (2020).
[14] M.S. Ho, J.H. Ri, S.B. Kim, Improved characteristic fast marching method for the generalized eikonal equation in a moving medium, J. Sci. Comput. 81 (3) (2019) 2484–2502.
[15] G. Huang, Q. Hu, S. Luo, H. Li, H. Zhang, D.C. Nobes, 2-d fast sweeping method for the factored eikonal equation and its improvement on inversion accuracy, J. Appl. Geophys. 166 (2019) 68–76.
[16] G. Huang, S. Luo, J. Deng, V. Vavryčuk, Traveltime calculations for qp, qsv, and qsh waves in two-dimensional tilted transversely isotropic media. Journal of Geophysical Research: Solid, Earth 125 (8) (2020), e2019JB018868.
[17] Huang, X.: Modeling and inversion of seismic data using multiple scattering, renormalization and homotopy methods (2020).
[18] A. Hutzler, C. Matthus, M. Rommel, L. Frey, Generalized approach to design multi-layer stacks for enhanced optical detectability of ultrathin layers, Applied physics letters 110 (2) (2017) 021909.
[19] R. Jiwari, R. Gupta, V. Kumar, Polynomial differential quadrature method for numerical solutions of the generalized fitzhugh–nagumo equation with time-dependent coefficients, Ain Shams Engineering Journal 5 (4) (2014) 1343–1350.
[20] D. Kabat, M. Ortiz, Eikonal quantum gravity and planckian scattering, Nucl. Phys. B 388 (2) (1992) 570–592.
[21] C.Y. Kao, S. Osher, Y.H. Tsai, Fast sweeping methods for static hamilton–jacobi equations, SIAM journal on numerical analysis 42 (6) (2005) 2612–2632.
[22] P. Le Bouteiller, M. Benjemaa, L. Métivier, J. Virieux, An accurate discontinuous galerkin method for solving point-source eikonal equation in 2-d heterogeneous anisotropic media, Geophys. J. Int. 212 (3) (2018) 1498–1522.
[23] R. Leach, Coordinate metrology. Fundamental Principles of Engineering Nanometrology, Elsevier, Oxford, 2010, pp. 263–288.
[24] M. Lehujeur, S. Chevrot, Eikonal tomography using coherent surface waves extracted from ambient noise by iterative matched filtering–application to the large-n maupasacq array. Journal of Geophysical Research: Solid, Earth 125 (6) (2020), e2020JB019363.
[25] M. Lehujeur, S. Chevrot, On the validity of the eikonal equation for surface-wave phase-velocity tomography, Geophys. J. Int. 223 (2) (2020) 908–914.
[26] H. Li, S.S. Mulay, Meshless methods and their numerical properties, CRC Press, 2013.
[27] W. Li, J. Qian, Newton-type gauss–seidel lax–friedrichs high-order fast sweeping methods for solving generalized eikonal equations at large-scale discretization, Computers & Mathematics with Applications 79 (4) (2020) 1222–1239.
[28] J.G. Liu, M. Osman, W.H. Zhu, L. Zhou, G.P. Ai, Different complex wave structures described by the hirota equation with variable coefficients in inhomogeneous optical fibers, Appl. Phys. B 125 (9) (2019) 1–9.
[29] O.H. Mohammed, M.A. Saeed, Numerical solution of thin plates problem via differential quadrature method using g-spline, Journal of King Saud University-Science 31 (2) (2019) 209–214.
[30] Ngondiep, E.: A novel three-level time-split maccormack method for solving two-dimensional viscous coupled burgers equations. arXiv preprint arXiv:1906.01544 (2019).
[31] M. Osman, New analytical study of water waves described by coupled fractional variant boussinesq equation in fluid dynamics, Pramana 93 (2) (2019) 1–10.
[32] M. Osman, D. Baleanu, A. Adem, K. Hosseini, M. Mirzazadeh, M. Eslami, Double-wave solutions and lie symmetry analysis to the (2 + 1)-dimensional coupled burgers equations, Chinese Journal of Physics 63 (2020) 122–129.

[33] M. Osman, D. Lu, M. Khater, R. Attia, Complex wave structures for abundant solutions related to the complex ginzburg–landau model, Optik 192 (2019) 162927.
[34] M. Osman, D. Lu, M.M. Khater, A study of optical wave propagation in the nonautonomous schrödinger-hirota equation with power-law nonlinearity, Results in Physics 13 (2019) 102157.
[35] L. Pedram, D. Rostamy, Numerical solutions of the initial boundary value problem for the perturbed conformable time korteweg-de vries equation by using the finite element method, Numerical Methods for Partial Differential Equations 37 (2) (2021) 1449–1463.
[36] Y. Pinchover, J. Rubinstein, An introduction to partial differential equations, Cambridge University Press, 2005.
[37] S. Qasemi, D. Rostamy, New local discontinuous galerkin method for a fractional time diffusion wave equation, International Journal of Computer Mathematics 96 (9) (2019) 1818–1838.
[38] S. Qasemi, D. Rostamy, N. Abdollahi, The time-fractional diffusion inverse problem subject to an extra measurement by a local discontinuous galerkin method, BIT Numerical Mathematics 59 (1) (2019) 183–212.
[39] H. Rezazadeh, M. Osman, M. Eslami, M. Mirzazadeh, Q. Zhou, S.A. Badri, A. Korkmaz, Hyperbolic rational solutions to a variety of conformable fractional boussinesq-like equations, Nonlinear Engineering 8 (1) (2019) 224–230.
[40] D. Rostamy, The new streamline diffusion for the 3d coupled schrodinger equations with a cross-phase modulation, ANZIAM Journal 55 (2013) E51–E78.
[41] M. Seike, N. Kawabata, M. Hasegawa, Quantitative assessment method for road tunnel fire safety: Development of an evacuation simulation method using cfd-derived smoke behavior, Safety science 94 (2017) 116–127.
[42] P. Sharma, Efficacy of harmonic differential quadrature method to vibration analysis of fgpm beam, Compos. Struct. 189 (2018) 107–116.
[43] C. Shu, Application of differential quadrature method to simulate natural convection in a concentric annulus, Int. J. Numer. Meth. Fluids 30 (8) (1999) 977–993.
[44] C. Shu, Differential quadrature and its application in engineering, Springer Science & Business Media, 2012.
[45] C. Shu, W. Chen, H. Xue, H. Du, Numerical study of grid distribution effect on accuracy of dq analysis of beams and plates by error estimation of derivative approximation, Int. J. Numer. Meth. Eng. 51 (2) (2001) 159–179.
[46] C. Shu, B. Khoo, Y. Chew, K. Yeo, Numerical studies of unsteady boundary layer flows past an impulsively started circular cylinder by gdq and giq approaches, Computer methods in applied mechanics and engineering 135 (3–4) (1996) 229–241.
[47] C. Shu, B.E. Richards, Application of generalized differential quadrature to solve two-dimensional incompressible navier-stokes equations, Int. J. Numer. Meth. Fluids 15 (7) (1992) 791–798.
[48] H. Srivastava, D. Baleanu, J. Machado, M. Osman, H. Rezazadeh, S. Arshed, H. Günerhan, Traveling wave solutions to nonlinear directional couplers by modified kudryashov method, Phys. Scr. 95 (7) (2020) 075217.
[49] G. Wang, X. Zhang, J. Cheng, A unified shape-from-shading approach for 3d surface reconstruction using fast eikonal solvers, International Journal of Optics 2020 (2020).
[50] S. Xu, A. Stovas, T. Alkhalifah, H. Mikada, New acoustic approximation for transversely isotropic media with a vertical symmetry axis, Geophysics 85 (1) (2020) C1–C12.
[51] S.G. Xu, Y.X. Zhang, J.H. Yong, A fast sweeping method for computing geodesics on triangular manifolds, IEEE transactions on pattern analysis and machine intelligence 32 (2) (2008) 231–241.
[52] U. Yücel, Approximations of sturm–liouville eigenvalues using differential quadrature (dq) method, J. Comput. Appl. Math. 192 (2) (2006) 310–319.
[53] U. Yücel, K. Boubaker, Differential quadrature method (dqm) and boubaker polynomials expansion scheme (bpes) for efficient computation of the eigenvalues of fourth-order sturm–liouville problems, Appl. Math. Model. 36 (1) (2012) 158–167.
[54] Y.T. Zhang, H.K. Zhao, J. Qian, High order fast sweeping methods for static hamilton–jacobi equations, J. Sci. Comput. 29 (1) (2006) 25–56.
[55] Z. Zhao, J. Chen, M. Wang, Comparison of the fast sweeping and fast marching methods for first-arrival p-wave traveltime calculation in attenuating vti media, J. Seismic Explorat. 29 (5) (2020) 403–424.